Solar Energy Materials & Solar Cells 93 (2009) 1618–1623

Contents lists available at ScienceDirect

Solar Energy Materials & Solar Cells

journal homepage: www.elsevier.com/locate/solmat

8 MeV electron irradiation studies on electrical characteristics of Cu(In,Ga)Se_2 solar cells

Asha Rao [a,*], Sheeja Krishnan [b], Ganesh Sanjeev [b], K. Siddappa [c], Harin S. Ullal [d], Xuanzhi Wu [d]

[a] Department of Physics, Mangalore Institute of Technology and Engineering, Moodabidri, Mangalore 574 227, India
[b] Microtron Centre, Department of Physics, Mangalore University, Mangalagangothri 574 199, India
[c] JSS Foundation for Science and Society, Bangalore 560 085, India
[d] National Center for Photovoltaics, National Renewable Energy Laboratory, 1617, Cole Boulevard, Golden, CO 80401, USA

ARTICLE INFO

Article history:
Received 9 January 2009
Received in revised form
26 April 2009
Accepted 28 April 2009
Available online 4 June 2009

Keywords:
CIGS
Solar cell
Electron irradiation
Current–voltage characteristics
Ideality factor
Series resistance
Capacitance–frequency
Efficiency

ABSTRACT

Cu(In,Ga)Se_2 (CIGS) solar cells are gaining considerable interest due to their high optical absorption coefficient and adjustable band gap, which enables them to achieve high conversion efficiency and also present many promising applications in space power systems. In this paper we report the results of the effect of temperature and 8 MeV electron irradiation on the electrical characteristics of ZnO/CdS/Cu(In,Ga)Se_2/Mo polycrystalline thin-film solar cells under forward and reverse bias studied in the temperature range 270–315 K. The solar cells were subjected to 8 MeV electron irradiation from the Microtron accelerator and were exposed to graded doses of electrons up to 75 kGy. *I–V* characteristics of the cells under dark and AM 1.5 illumination condition were studied before and after the irradiation. Capacitance measurements were also carried out at various frequencies before and after irradiation. In the measured temperature range, the dark current contribution is due to the generation–recombination of the minority carriers in the depletion region. The ideality factor is found to decrease with increase in temperature. It seems that electron irradiation has not altered the dark current conduction mechanism significantly. The effect of electron irradiation on the solar cell parameters such as fill factor (FF), conversion efficiency (η), saturation current (I_o), short circuit current (I_{sc}), open circuit voltage (V_{oc}), and ideality factor (n) was studied. They were found to be stable up to 75 kGy of electron dose as only small changes were observed in the solar cell parameters.

1. Introduction

Cu(In,Ga)Se_2 (CIGS) thin-film solar cells present many promising applications in space power systems. With the development of thin-film solar cells for terrestrial applications, there is an interest in transitioning this technology to space applications. CIGS thin-film solar cells have been fabricated by several research groups at over 15% efficiency, and the efficiency record obtained for a small laboratory cell is as high as 19.9% as found by NREL scientists [1]. Laboratory mini-modules have reached 16.6% efficiency [2]. The CIGS/CdS solar cell has demonstrated the highest efficiency of 19% among thin-film solar cells [3]. CIGS devices have shown promising results in outdoor long-term performance tests [4], but at the same time they are more sensitive than crystalline silicon solar cells to hot and humid environments [5]. Successful application of the devices in the advanced space-borne systems demand characterization of cell properties like dark current under different ambient conditions and the stability of the cells against particle irradiation in space [6,7]. Investigations show that the cell efficiency decreases under proton and electron irradiation, because the semiconductor properties get changed by introduction of defects [8]. CIGS thin-film solar cells have shown outstanding hardness against high-energy electron irradiation. An end-of-life efficiency of 13.4% under standard AM0 illumination has been reported for CIGS thin-film solar cells after irradiating with 1 MeV electrons after $\phi_e = 5 \times 10^{16}\,cm^{-2}$ [9]. CIGS solar cells irradiated with 1 MeV electron fluence of $10^{18}\,cm^{-2}$ degrade to about 80% of their initial conversion efficiency [10]. Irradiation experiments on CIGS thin-film solar cells with 3 MeV electrons cause a degradation of the short circuit current ISC starting at fluences $\phi_e = 2 \times 10^{17}\,cm^{-2}$ and leading to a loss of 90% of the initial I_{sc} at $\phi_e = 2 \times 10^{18}\,cm^{-2}$ [11]. The electrical behavior and the performance of CIGS solar cells seem to be influenced mainly by the defect levels located at the CdS/CIGS interface and in the depletion region. Thus, in order to improve device properties of these heterojunction solar cells, the characterization of these levels is necessary. Hence more attention is given to the processes at the interfaces of these devices that take place during

* Corresponding author. Tel.: +91 824 2232251.
E-mail address: asha_rao_i@yahoo.com (A. Rao).

0927-0248/$ - see front matter © 2009 Elsevier B.V. All rights reserved.
doi:10.1016/j.solmat.2009.04.021

the junction formation and also during particle irradiation and the powerful electrical consequences of these interactions [6]. In the present work, solar cell properties were studied by *I–V* measurements under dark condition in the temperature range 250–315 K and under AM1.5 illumination condition before and after irradiation with graded doses of 8 MeV electrons up to 75 kGy with an intention to understand the different aspects of dark current transport and also to test the stability of CIGS solar cells against 8 MeV electron irradiation and the results are analyzed.

2. Experimental

The CIGS solar cell samples S2230-A1 and S2230-B1 with area 0.430 cm^2 used in the present study were fabricated by co-evaporation of the elements Cu, In, Ga, and Se, on a molybdenum-coated soda lime glass using a bi-layer process [12]. Molybdenum acts as back contact. Heterojunction formation via chemical bath deposition of CdS and subsequent sputter deposition of Al-doped ZnO, having good optical and electrical properties, acts as a good front contact for the CIGS solar cell samples. The absorber layer thickness is typically between 1 and 1.5 μm. Heterojunction formation via chemical bath deposition of approximately 50 nm CdS and sputter deposition of 70 nm undoped and 300 nm Al-doped ZnO followed by evaporation of an Al metal grid finalizes the device process. The samples used here have a mean initial efficiency between 15.5% and 14% and an initial open circuit voltage between 0.59 and 0.64 V. The temperature-dependent dark *I–V* characteristics of the samples were studied under both forward and reverse bias in the temperature range 250–315 K. *I–V* characteristics of solar cells under illumination were measured at room temperature using a computer-controlled Keithley 236 SMU. The cells were illuminated under AM1.5 condition. The intensity of the light source was adjusted to 100 mW cm^{-2} using a light intensity meter Suryamapi. Capacitance measurements of the devices at various frequencies were also carried out under dark condition using a Keithley 3322 LCZ meter. Solar cell samples were irradiated at room temperature with 8 MeV electrons from a Microtron accelerator. The features of the Microtron are detailed elsewhere [13,14]. The cells were exposed to electrons of doses ranging from 1 to 75 kGy. The *I–V* characteristics were measured both under dark condition in the temperature range 250–315 K and under AM1.5 condition, and capacitance–frequency measurement is done at room temperature. These measurements were repeated for the solar cell samples after the irradiation. Both the samples showed almost similar characteristics and same response to the electron irradiation. Hence the results of the solar cell sample S2230-A1 is presented in this article.

3. Results and discussion

3.1. Forward dark I–V characteristics

Current–voltage characteristics of a p–n junction is described by the expression

$$I = I_s \exp(qV/nkT) \quad (1)$$

where n is the ideality factor, I_s the saturation current, k the Boltzmann constant and T the temperature. An accurate knowledge of the ideality factor as a function of temperature is of vital importance for the characterization of current transport mechanisms and interfacial properties. The ideality factor and the saturation current are calculated from the *I–V* plots by fitting the data to Eq. (1). The ideality factor n is equal to 1 if the diffusion current dominates and is equal to 2 when generation and recombination of the electron–hole pairs in the junction depletion region dominates [15]. The forward *I–V* characterization of the CIGS solar cell sample, after irradiating with electrons for a dose of 75 kGy, was carried out over a temperature range of 250–315 K. Fig. 1a and b shows the semi-logarithmic forward dark *I–V* plots at various temperatures for the unirradiated and irradiated CIGS solar cell sample. It is observed in both the cases that the dark current in CIGS solar cell increases exponentially with the increase in bias voltage. The ideality factor is calculated from the slope of the straight-line regions of plot drawn with log dark *I* against *V*. The value of n between 3.0 for 250 K and 2.1 for 290 K suggests that the dark current is due to the generation–recombination of charge carriers at the interface.

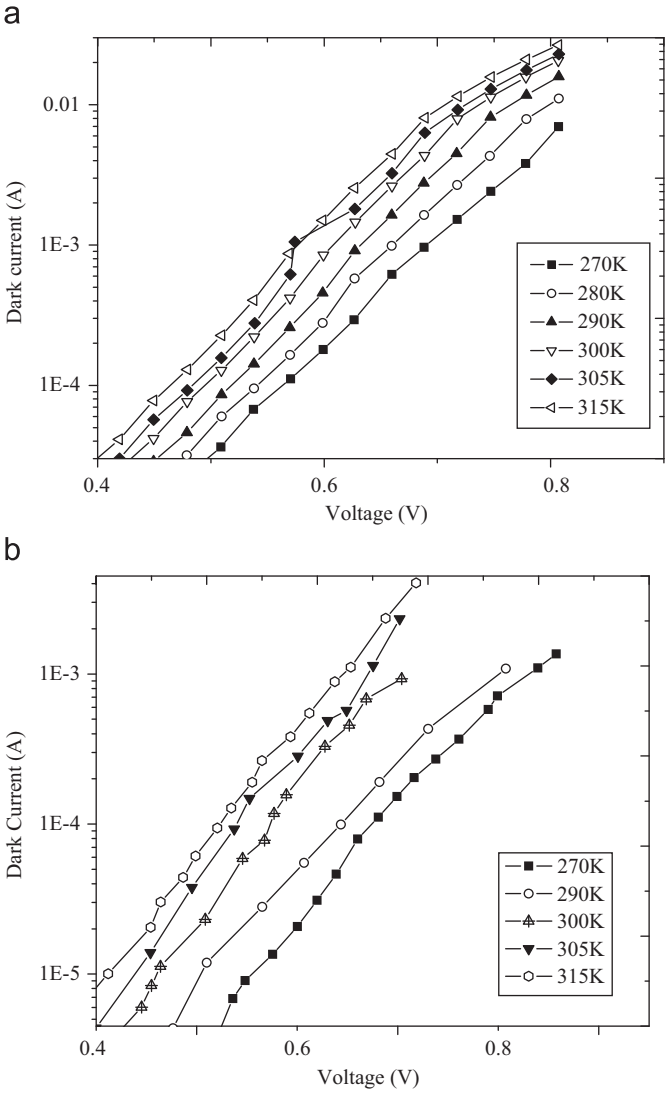

Fig. 1. (a) The semi-logarithmic forward dark *I–V* plots of (a) unirradiated CIGS Solar cell sample S2230-A1 at various temperatures and (b) irradiated CIGS Solar cell sample S2230-A1 with electrons of dose 75 kGy at various temperatures.

The variation of ideality factor of unirradiated and irradiated CIGS solar cell sample S2230-A1 as a function of temperature is shown in Fig. 2. A small increase in the ideality factor is seen after irradiation and is found to decrease with increase in temperature. This is because increasing temperature increases the thermal movement of the atoms in the material, thereby enhancing the recombination within the bulk of the material. Decrease in the ideality factor may also be caused by the increase of saturation current I_S, which is due to the modification of the current

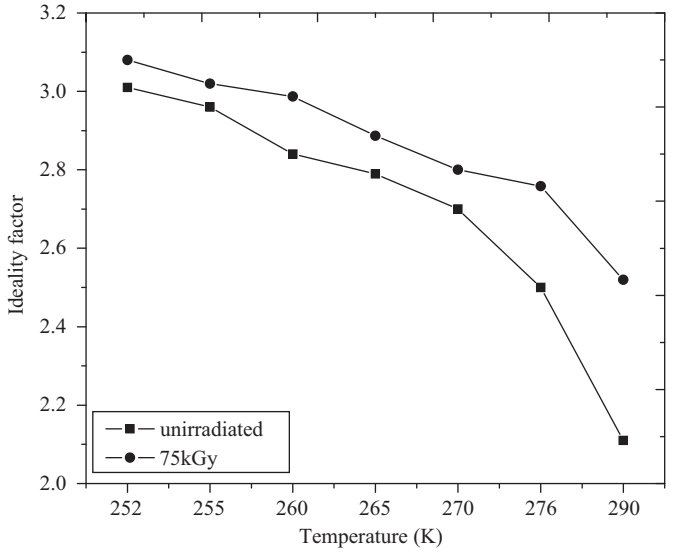

Fig. 2. The variation of ideality factor of unirradiated and irradiated CIGS solar cell sample S2230-A1 as a function of temperature.

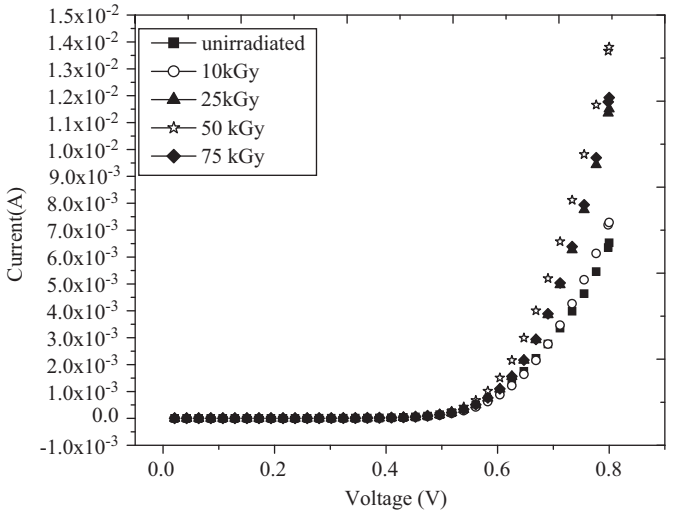

Fig. 4. Forward *I–V* characteristics of the CIGS solar cell sample S2230-A1 under dark condition at various doses of 8 MeV electrons.

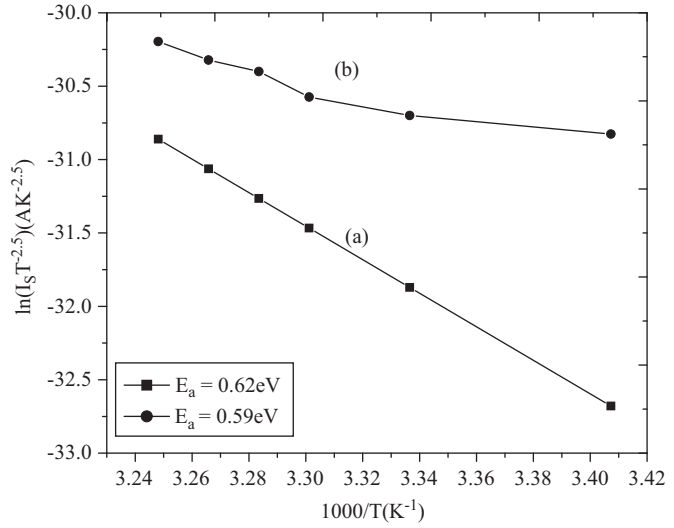

Fig. 3. The plot of $\ln(I_sT^{-2.5})$ versus $1000/T$ for CIGS solar cell sample S2230-A1 in the temperature range 290–310 K: (a) unirradiated and (b) irradiated with electrons of dose 75 kGy.

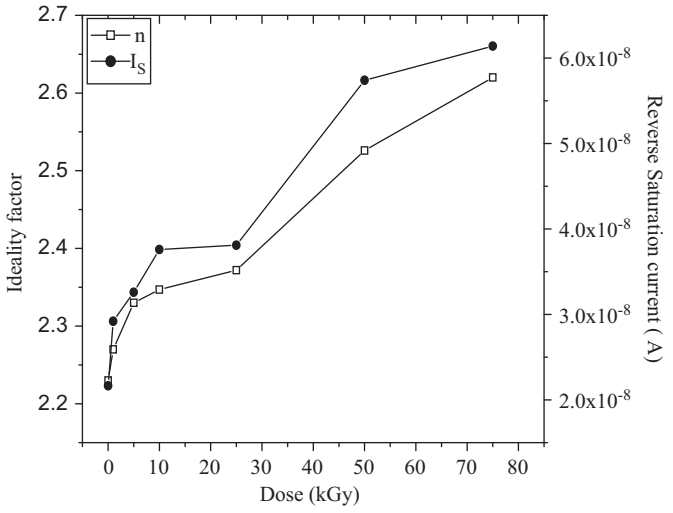

Fig. 5. The variation of reverse saturation current and the ideality factor of CIGS solar cell sample S2230-A1 at various doses of 8 MeV electrons.

transport mechanism in the device. The decrease in diode ideality factors can thus be interpreted as a relative increase of recombination in the bulk of the material as compared with the recombination in the space charge region [16].

A plot of $\ln(I_sT^{-2.5})$ versus $1/T$ for unirradiated and irradiated CIGS solar cell sample S2230-A1 in the temperature range 290–310 K is shown in Fig. 3. The activation energy determined from such a plot should be equal to approximately half the band gap if the current is controlled by the generation–recombination in the depletion region [17–20] and it should be close to the band gap if the current is controlled by diffusion [19,20]. The activation energy calculated from the slope of the $\ln(I_sT^{-2.5})$ versus $1000/T$ is found to be 0.62 eV before irradiation and 0.59 eV after irradiation with electrons at a dose of 75 kGy. Activation energy calculated in both the cases is found to be nearly equal to half the band gap of CIGS. This suggests that the generation–recombination of the carriers in the depletion region determines the dark current. It is found that there is only slight change in the current after irradiation, suggesting that there is no major change in the depletion region of the device by electron irradiation. Even though the primary defects are formed by electron irradiation, they might have been swept away before they formed the stable complex defects. Fig. 4 represents the forward dark *I–V* characteristics of the CIGS solar cell sample S2230-A1 irradiated with different electron doses. The variation of saturation current and the ideality factor with different electron doses are shown in Fig. 5. No significant variation is found even at a dose of 75 kGy. It is well known that recombination centers introduced by electron irradiation decrease the minority carrier diffusion length, and at low doses of electron irradiation, the degradation is due to the decrease in minority carrier diffusion length [21]. The device series resistance in the dark was determined from the inverse of the slope of *I–V* characteristics. It is observed that series resistance increases with increase in electron dose. The increase in series resistance might be due to the carrier removal observed with irradiation.

3.2. Reverse I–V characteristics

The reverse dark *I–V* characteristics of the CIGS solar cell at various temperatures and at various electron doses are studied systematically. It is found that the reverse current does not show any saturation in the whole applied voltage range. This indicates that the dark current is governed by generation–recombination of carriers in the depletion region. Fig. 6 shows the Arrhenius plot [$\log(I_R)$ versus $1000/T$] for unirradiated and irradiated solar cell sample S2230-A1. As the Arrhenius plot appears to exhibit thermally activated behavior, the reverse current can be expressed as

$$I_R(T) \propto \exp(-E_a/kT) \quad (2)$$

where E_a is the activation energy and k the Boltzmann constant [15].

The activation energy determined from such a plot should be equal to approximately half the band gap if the current is controlled by generation–recombination in the depletion region [15,22]. The activation energy calculated from the Arrhenius plot at −0.7 V is 0.58 eV before irradiation and 0.56 eV after irradiation. Both these values are close to half the band gap of CIGS. This suggests that the generation–recombination of carriers in the depletion region that determines the dark current has not changed much after electron irradiation.

3.3. I–V characteristics under illumination

Fig. 7 shows the illuminated *I–V* characteristics of the CIGS solar cell sample S2230-A1 subjected to graded electron doses up to 75 kGy, under AM1.5 illumination condition. The solar cell parameters like open circuit voltage (V_{oc}), short circuit current (I_{sc}), fill factor (FF) and efficiency were calculated from the *I–V* characteristics.

The current flowing in a solar cell under illumination is given by [15]

$$I = I_o[\exp(qV/nkT) - 1)] - I_L \quad (3)$$

where n is the diode ideality factor, I_o the dark saturation current of the CdS/CIGS junction, n the diode ideality factor and I_L the photo-generated current in the CIGS layer.

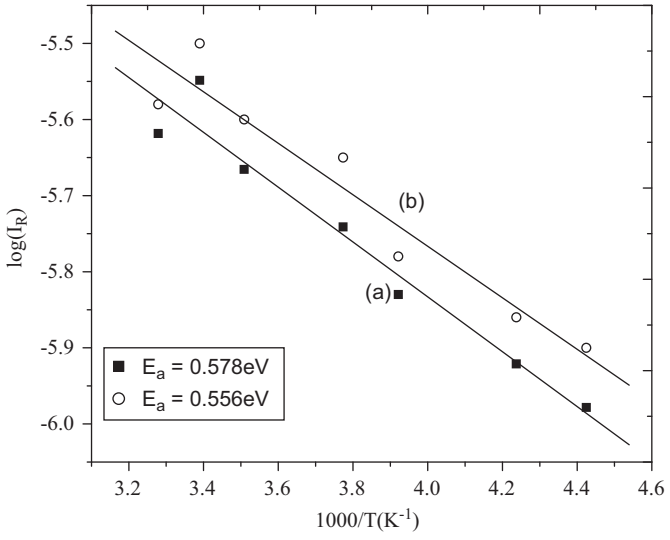

Fig. 6. Arrhenius plot of the reverse current of a CIGS solar cell sample S2230-A1 at a bias of −0.7 V: (a) unirradiated and (b) irradiated with electrons of 75 kGy.

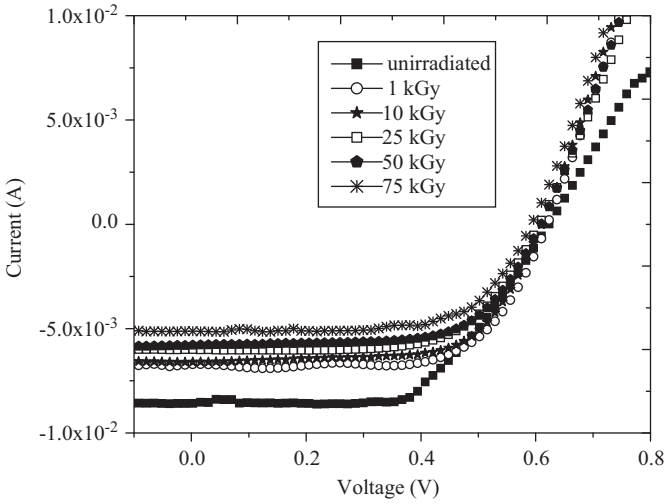

Fig. 7. *I–V* characteristics of CIGS solar cell sample S2230-A1 at various doses of 8 MeV electrons under AM 1.5 illumination condition.

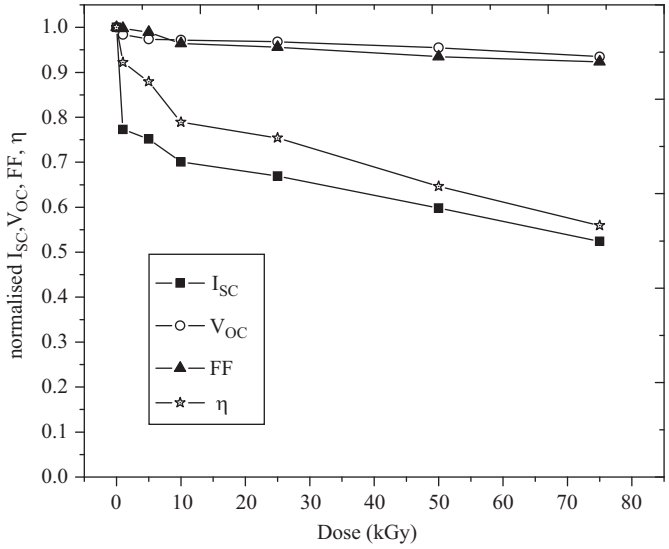

Fig. 8. Normalized solar cell parameters as a function of dose.

The open circuit voltage is related to the saturation current given by [15]

$$V_{oc} = (nkT/q)\ln[(I_{sc}/I_o) + 1] \quad (4)$$

It can be seen that V_{oc} depends on the properties of the semiconductor by virtue of its dependence on I_o.

Fill factor of the solar cell is defined by [15]

$$FF = (V_{MP}I_{MP})/(V_{OC}I_{SC}) \quad (5)$$

where I_{MP} and V_{MP} are the current and voltage at the maximum power point on the *I–V* curve.

The energy conversion efficiency of a solar cell can be written as [15]

$$\eta = I_{MP}V_{MP}/P_{in}A \quad (6)$$

where P_{in} is the incident solar power density and A the area of the solar cell.

Fig. 8 shows the changes in the solar cell parameters of the CIGS solar cell sample S2230-A1 normalized to their initial value, as a function of electron dose. A remarkable reduction in the short circuit current and efficiency is observed with increase in electron dose. There is no considerable variation in the fill factor and the

open circuit voltage. Even after electron irradiation for 75 kGy the normalized values of FF and V_{OC} remain at 92% and 93%, respectively. The decrease in the efficiency of the solar cell is mainly because of the decrease in the values of I_{SC}. The decrease in the short circuit current may be because of decrease in the minority carrier diffusion length due to the introduction of radiation-induced defects.

3.4. Capacitance–frequency measurements

The variation of capacitance with frequency is used to determine the density of interface states in the devices. In general, interface states in equilibrium with the semiconductor do not contribute to the capacitance at sufficiently high frequencies. At low frequencies, the contribution of the interface states to device capacitance decreases with increase in frequency. Measured capacitance at low frequency is approximately equal to the sum of the space charge capacitance (C_{sc}) and the interface capacitance (C_{ss}), which at high frequencies is equal to space charge capacitance only [23]. Thus at a given bias, the values of the capacitance in a high-frequency region are subtracted from the experimental junction capacitance C, yielding the interface state capacitance C_{ss}.

Variation of the interface state capacitance C_{ss} with frequency is given by [24]

$$C_{ss} = AqN_{ss} \arctan(\omega\tau)/\omega\tau \quad (7)$$

The variation of capacitance with frequency for CIGS solar cell sample S2230-A1 irradiated with 8 MeV electrons was studied under dark conditions at 1 V. The capacitance is found to decrease with increase in frequency, indicating the presence of deep levels near the CdS/CIGS interface. The capacitance value varied from 8.9 to 2.8 nF for the frequency variation of 100 Hz to 100 kHz, for the unirradiated sample. The corresponding decrease in the capacitance value for the device irradiated with electron of dose 75 kGy is from 8.8 to 2.6 nF. The decrease in the capacitance values of irradiated and unirradiated samples is not too large, indicating that electron irradiation has not contributed significantly to the concentration of deep level defects. The interface trap concentrations before and after irradiation were 1.07×10^{13} and 1.10×10^{12} $eV^{-1}\,cm^{-2}$ (Eq. (7)), indicating that irradiation has not contributed significantly to the concentration of the deep level defects.

4. Conclusion

The dark current of CIGS solar cell samples S2230-A1 and S2230-B1 as a function of temperature and applied voltage and also the effect of 8 MeV electron irradiation on the properties of CIGS solar cell samples under dark and illumination conditions have been studied and the following conclusions were drawn.

(1). No major change is observed in the dark current after electron irradiation, suggesting that the depletion region of the device has not been affected much by electron irradiation. But it can be concluded that continuous irradiation with 8 MeV electrons to the devices at various temperatures will significantly affect the dark current. The ideality factor is found to decrease with increase in temperature because of increase in the thermal movement of atoms enhancing the recombination within the material and also due to the relative increase of recombination in the bulk of the material as compared with the recombination in the space charge region.

(2). The decrease in the efficiency of the solar cell after electron irradiation is mainly because of the decrease in the values of I_{SC}. The decrease in the short circuit current may be due to decrease in the minority carrier diffusion length because of the introduction of radiation-induced defects.

(3). Capacitance variation with frequency indicates that electron irradiation has not contributed significantly to the increase of deep level defects. But continuous irradiation with 8 MeV electrons to the devices will significantly contribute to the variation in the electrical characteristics.

Acknowledgements

The authors are grateful to the the Staff and Research Scholars of Microtron Centre, Mangalore University, for their help and support during irradiation. The authors thank Professor Shiv Kumar, NITK, for extending facilities for capacitance studies. One of the authors (AR) gratefully acknowledges the support and encouragement given by the management and staff of Mangalore Institute of Technology and Engineering, Moodbidri.

References

[1] M.A. Contreras, B. Egaas, K. Ramanathan, J. Hiltner, A. Swartzlander, F. Hasoon, R. Noufi, Progress toward 20% efficiency in Cu (In,Ga)Se_2 polycrystalline thin-film solar cells, Prog. Photovoltaics: Res. Appl. 7 (1999) 311–316.
[2] J. Kessler, M. Bodegard, J. Hedstrom, L. Stolt, New world record Cu(In,Ga)Se_2 based mini-module: 16.6%, in: Proceedings of the 16th European Photovoltaic Solar Energy Conference, 2000, pp. 2057–2060.
[3] K. Ramanathan, M.A. Contreras, C.L. Perkins, S. Asher, F.S. Hasoon, J. Keane, D. Young, M. Romero, W. Metzger, R. Noufi, J. Ward, A. Duda, Properties of 19.2% efficiency ZnO/CdS/CuInGaSe_2 thin-film solar cells, Prog. Photovoltaics: Res. Appl. 11 (2003) 225–230.
[4] H.S. Ullal, K. Zweibel, B.G. Von Roedern, Polycrystalline thin film photovoltaics: research, development, and technologies, in: Proceedings of the 26th IEEE Photovoltaic Specialists Conference, 1997, pp. 301–305.
[5] F. Karg, H. Calwer, J. Rimmasch, V. Probst, W. Riedl, W. Stetter, H. Vogt, M. Lampert, Development of procedures for performance measurements and lifetime testing of thin film photovoltaic devices, Proc. Inst. Phys. Conf. 152 (1998) 909–913.
[6] P. Iles, Future of photovoltaics for space applications, Prog. Photovoltaics: Res. Appl. 8 (2000) 39–51.
[7] N. Dhere, S. Ghongadi, M. Pandit, A. Jahagirdar, D. Scheiman, $CIGS_2$ thin-film solar cells on flexible foils for space power, Prog. Photovoltaics: Res. Appl. 10 (2002) 407–416.
[8] A. Jasenek, U. Rau, Defect generation in Cu(In,Ga)Se_2 heterojunction solar cells by high-energy electron and proton irradiation, J. Appl. Phys. 90 (2001) 650–658.
[9] A. Jasenek, T. Hahn, M. Schmidt, K. Weinert, M. Wimbor, G. Hanna, K. Orgassa, M. Hartmann, H.W. Schock, U. Rau, J.H. Werner, B. Schattat, S. Kraft, K.H. Schmid, W. Bolse, G. La Roche, A. Robben, K Bogus, Radiation induced defects in Cu (In,Ga)Se_2 solar cells—comparison of electron and proton irradiation, in: Proceedings of the 16th Photovoltaic Solar Energy Conference and Exhibition, 2000, pp. 982–985.
[10] A. Jasenek, U. Rau, K. Weinert, I.M. Kötschau, G. Hanna, G. Voorwinden, M. Powalla, H.W. Schock, J.H. Werner, Radiation resistance of Cu (In,Ga)Se_2 solar cells under 1-MeV electron irradiation, Thin Solid Films 387 (1–2) (2001) 228–230.
[11] K. Weinert, A. Jasenek, U. Rau, Consequence of 3-MeV electron irradiation on the photovoltaic output parameters of Cu(In,Ga)Se_2 solar cells, Thin Solid Films 431–432 (2003) 453–458.
[12] L. Stolt, J. Hedstrom, J. Kessler, M. Ruckh, K.O. Velthaus, H.W. Schock, ZnO/CdS/$CuInSe_2$ thin film solar cells with improved performance, Appl. Phys. Lett. 62 (1993) 597–599.
[13] K. Siddappa, Ganesh, S.S. Ramamurthy, H.C. Soni, P. Srivastava, Y. Sheth, Hemnani, Variable energy microtron for R & D work, Radiat. Phys. Chem. 51 (4–6) (1998) 441–442.
[14] Ganesh, K.C. Prashanth, Y.N. Nagesh, A.P. GnanaPrakash, D. Umakanth, M. Pattabi, K. Siddappa, S. Salkalachen, A. Roy, Modification of power diode characteristics using bremsstrahlung radiation from microtron, Radiat. Phys. Chem. 55 (1999) 461–464.
[15] S.M. Sze, Physics of Semiconductor Devices, 2nd ed., Wiley Interscience, New York, 1981, pp. 807–808.
[16] W.A. Miller, L.O. Olsen, Current transport in boeing (Cd,Zn)S/$CuInSe_2$ solar cells, IEEE Trans. Electr. Dev. Ed. 31 (1984) 654–656.
[17] J.B. Yoo, A.L. Fahrenbruch, R.H. Bube, Transport mechanisms in ZnO/CdS/$CuInSe_2$ solar cells, J. Appl. Phys. 68 (1990) 4694–4699.
[18] A. Ringe, A.W. Smith, M.H. MacDougal, A. Rohatgi, The effects of $CdCl_2$ on the electronic properties of molecular-beam epitaxially grown CdTe/CdS heterojunction solar cells, J. Appl. Phys. 70 (1991) 881–890.

[19] A. Zemel, I. Lukomsky, E. Weiss, Mechanism of carrier transport across the junction of narrow band-gap planar n+p HgCdTe photodiodes grown by liquid-phase epitaxy, J. Appl. Phys. 98 (2005) 054504–054507.
[20] H. Bayhen, C. Ercelebi, Electrical characterization of vacuum-deposited n-CdS/p-CdTe heterojunction devices, Semicond. Sci. Technol. 12 (1997) 600–604.
[21] M. Yamaguchi, S.J. Taylor, M.J. Yang, S. Matsuda, O. Kawasaki, T. Hisamatsu, High-energy and high-fluence proton irradiation effects in silicon solar cells, J. Appl. Phys. 80 (9) (1996) 4916–4919.
[22] A. Czerwinski, E. Simoen, A. Povai, C. Claeys, Activation energy analysis as a tool for extraction and investigation of p–n junction leakage current components, J. Appl. Phys. 94 (2003) 1218–1221.
[23] E. Ayyildiz, L.C. Nuho, A. Turut, The determination of the interface-state density distribution from the capacitance–frequency measurements in Au/n-Si Schottky barrier diodes, J. Electron. Mater. 31 (2002) 119–123.
[24] A. Singh, Characterization of interface states at Ni/$n$$CdF_2$ Schottky barrier type diodes and the effect of CdF_2 surface preparation, Solid State Electron. 28 (1985) 223–232.